

Analysis of Bending Effects on Performance Degradation of ITER-Relevant Nb₃Sn Strand Using the THELMA Code

R. Zanino, D. P. Boso, M. Lefik, P. L. Ribani, L. Savoldi Richard, and B. A. Schrefler

Abstract—The modeling of the effects of bending on single Nb₃Sn strand DC performance (I_C , n index) is presented for a bronze-route strand subjected to the same loading conditions as in an experiment performed at JAEA Naka, Japan [Y. Nunoya, *et al.*, *IEEE TAS 14* (2004) 1468–1472]. The strand is discretized in strand elements (SE) representing groups of twisted filaments in the bronze matrix, and in portions of the outer Cu annulus, electro-magnetically coupled in the THELMA code. The 3-D strain map in the filament region is computed with a newly developed, detailed thermo-mechanical model accounting for non-linear, temperature dependent material characteristics. With respect to our previous analysis [P.L.Ribani, *et al.*, *IEEE TAS 16* (2006) 860–863] several new updated ingredients, besides the new thermo-mechanical model, are used here, including more accurate thermal and mechanical properties for the materials, a jacket-like model for the outer Cu layer, I_C and n index (interpolative) scaling from Durham University. The simulation results show an improved agreement with the experiments, in the degradation of the single-strand performance due to bending.

Index Terms—Fusion reactors, ITER, modeling, superconducting filaments and wires.

I. INTRODUCTION

THE International Thermonuclear Experimental Reactor (ITER) is going to be built in Cadarache, France during the next 10 years and operated for another 20 years. It adopts a tokamak configuration with superconducting coils confining the plasma. The vast majority of the superconductors to be used in the coil system will be low critical temperature superconductors and for a big subset of the coils Nb₃Sn will be adopted.

Nb₃Sn presents, with respect to, e.g., NbTi, an issue related to the strain dependence of its critical performances. During the test of both ITER Central Solenoid and Toroidal Field Model Coils (CSMC and TFMC, respectively), an excellent result of the experiments was demonstrated, sometimes outperforming their original scope [1], [2], but an increasing degradation of the coil performance with respect to single strand was also noted at increasing electro-mechanical load [3]–[5]. This degradation

was hypothesized to be related to bending effects occurring inside the conductor [6], not included in the ITER design criteria at that time. Eventually, similar empirical correlations between degradation and load were also demonstrated on previously tested short samples [7]–[9], indicating a somewhat ubiquitous nature. As a consequence of all these observations and analyses, additional tests were performed both on single strands [10], [11] and on sub-size cables [12], aiming at elucidating the basic degradation effects for a single strand, as well as the possible effects of different cabling features (void fraction, twist pitches, etc) on the conductor performance. Also, new full-size ITER samples have been recently tested in the SULTAN facility [13], showing improved performance based on different cabling.

Analysis of the single strand bending tests was started some years ago, using different models: 1) a self-consistent thermo-mechanical model [14]–[17] following cool-down and load application on the strand combined with the distributed parameter electromagnetic model of a cable-in-conduit conductor [18] implemented in the THELMA code and applied in this case to the filament region in [19], 2) an ad hoc assumption on the thermal strain, combined with a beam model and a lumped parameter electromagnetic model for the strand, with ad hoc inter-filament conductance, in [20], [21].

Here we reconsider our previous work [19] on the experiments by Y. Nunoya at JAEA Naka, Japan, see Fig. 1, taking into account several new, improved ingredients now included in our model as follows:

- The new thermo-mechanical model described in Section II-A is developed and validated;
- New input data for the mechanical properties are used, derived from [21] and [22];
- The newly developed electromagnetic model of the jacket [23], summarized in Section III-A, is adopted for the outer Cu annulus;
- More accurate strand critical current (I_C) and critical exponent n interpolative scaling derived from Durham data [24], [25] are used, instead of the customary ITER-Summers scaling.

The general approach remains however as in [19]: the strain maps computed by the thermo-mechanical model are fed into the THELMA code to compute the critical current density, simulating I_C tests as performed in the experiment.

II. THERMO-MECHANICAL MODEL AND INPUT

A. New Features of the Thermo-Mechanical Model

Starting from a scanning electron microscope image of the Furukawa strand, see Fig. 1, a detailed Finite Element model

Manuscript received August 29, 2007. This work was supported in part by the Italian Ministry for University and Research (MUR).

R. Zanino and L. S. Richard are with Dipartimento di Energetica, Politecnico, I-10129 Torino Italy (e-mail: roberto.zanino@polito.it).

D. P. Boso and B. A. Schrefler are with Università di Padova, Italy.

M. Lefik is with Technical University of Łódź, Poland.

P. L. Ribani is with Università di Bologna, Italy.

Color versions of one or more of the figures in this paper are available online at <http://ieeexplore.ieee.org>.

Digital Object Identifier 10.1109/TASC.2008.921336

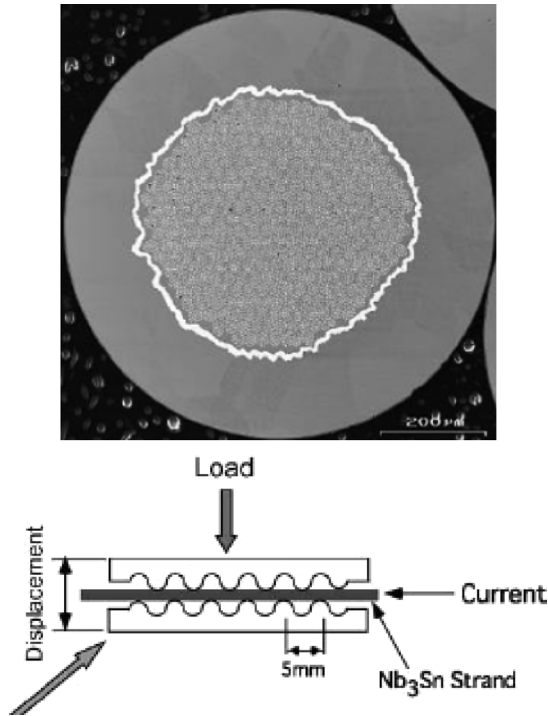


Fig. 1. Top: bronze-route (Furukawa) strand tested by Y. Nunoya at JAEA Naka, Japan (central filament region, Ta diffusion barrier, outer Cu annulus) Bottom: sketch of the experimental set-up. V-I characteristics were measured for several displacements.

has been developed, to take into account the exact area ratios ($\text{Cu}/\text{NonCu} = 1.464$, $\text{Nb}_3\text{Sn}/\text{bronze} = 0.557$) of the different materials in the strand cross section. The spatial discretization covers an entire bending period (5 mm) of the wire, and also the filament twisting is modeled (17.3 mm twist pitch). The mesh is composed of 3-D continuum elements, suitable to solve the problem in the coupled thermal-mechanical field. The number of nodes is 57022 for a total of 228987 degrees of freedom (displacement components and temperature). Particular attention was paid to reproduce the proper boundary conditions at the wire ends, to simulate the real configuration during the tests. Compared to our previous paper [19], this model is no more based on a *beam type* element, in order to be able to take into consideration in detail the strain field also in the cross section of the strand. In this manner the various components of the strain tensor are evaluated at all the integration points of the 464 elements present in the cross section, and the evolution of the plasticity is followed in a proper way. The von Mises yield criterion is adopted for these analyses.

B. New Features of the Thermo-Mechanical Input

New material characteristics have been used, mainly taken from [22]. The complete non linear behavior is considered, allowing reproducing the stress-strain curve of the materials for a set of 8 reference temperatures in the range from 1000 K to 4 K.

One of the major uncertainties in the thermo-mechanical input is the Sn content in the bronze matrix after heat treatment, which to the best of our knowledge was not measured so far for this strand. Different numerical tests were made, parametrically changing the Sn content in bronze from 5% to 1%. Also dif-

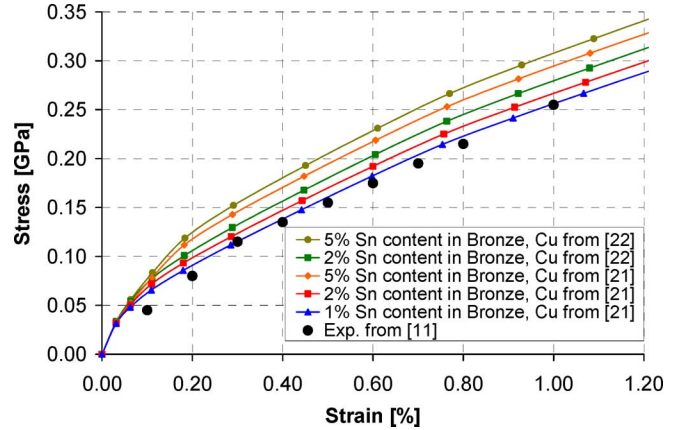


Fig. 2. Comparison between measured stress-strain characteristic under axial load and computed characteristics for different material properties.

ferent mechanical characteristics for Cu were used, including those measured at FzK as reported in [21].

C. Comparison With Experimental Data: Cool-Down Strain, Behavior Under Longitudinal Load

In this first set of analyses we simulate the cool down and a following applied axial tensile load, also to test the material thermal-mechanical data used in input.

The computed mechanical strain in Nb_3Sn filaments due to the cool down results (-0.42 ± 0.01)%, which may be compared with the (electromagnetically) measured value of $\sim -0.29\%$ [24]. The relative discrepancy could be related to uncertainties in the thermal expansion properties.

After the cool-down an axial displacement at one end of the wire is applied, to reproduce the stress strain curve measured at 4 K at the University of Twente [11]. This is a good experiment to test the mechanical data used, because only the axial stiffness is involved and the estimation of the area ratios was done rather precisely for this model. The comparison between the experimental and the numerical results is shown in Fig. 2. With the material characteristics taken from [22] the global behavior of the strand is still too stiff, even decreasing the Sn content to the minimum possible. However, assuming the Cu characteristics from [21], a very good agreement with the experimental test was obtained (blue triangle line).

D. Computed Bending Strain

After the validation of the material mechanical properties the JAEA experiment was simulated, performing the cool down and successively applying the bending load. The load is applied as a self-balanced volume force, varying parabolically on each half period along the length of the strand. The strain maps in the Nb_3Sn filaments were recorded as a function of the displacement of the strand axis in five representative cross sections, see inset in Fig. 3. Fig. 3 shows an example of strain map for a given displacement, while the minimum and maximum strain computed for the different displacements (always on section “0”) is reported in Table I.

III. ELECTROMAGNETIC MODEL AND INPUT

The strand is modeled adopting different discretizations of the *filament region* in strand elements (SE), i.e., bundles of fila-

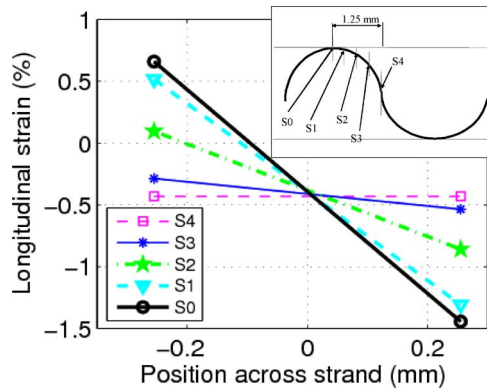


Fig. 3. Example of the computed strain maps as a function of the coordinate on the diameter x , at different cross sections along the strand as indicated, for the case of displacement $\delta = 53.7 \mu\text{m}$.

TABLE I
MAX-MIN COMPUTED BENDING STRAINS

Displacement (μm)	Max strain (%)	Min strain (%)
0	-0.42	-0.42
26.9	0.13	-0.90
53.7	0.66	-1.44
71.4	0.99	-1.78
101.6	1.54	-2.34

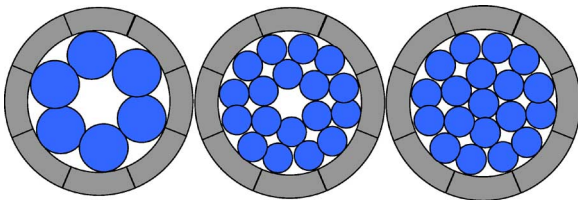


Fig. 4. Different discretizations of the strand cross section: From left to right number of filament bundles $N_{SE} = 6, 18, 19$. 8 resistive elements are used for the outer Cu annulus.

ments, and discretizing the outer Cu annulus as well, see Fig. 4. The present version of the code, developed originally for multi-stage cable-in-conduit conductors [18], cannot easily analyze arbitrary discretizations of the strand cross section, so that at present we are more-or-less restricted to those shown in the Figure.

A. New Features of the Electromagnetic Model

The major new feature of the electromagnetic model is the inclusion of the Cu outer annulus, described by means of the newly developed 3-D “jacket” model in THELMA [23]. The model calculates the current distribution in the jacket by solving a resistive distributed network, taking into account the exchange of current between SEs and jacket and the magnetic coupling with the cable and the external coil.

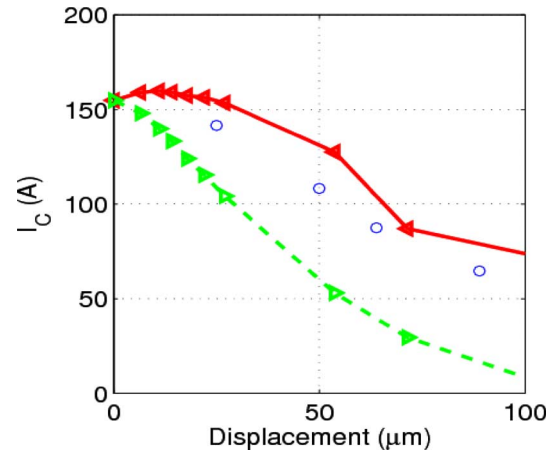


Fig. 5. Comparison of measured I_C (open circles) with the result of Ekin’s formulas [26] for the case of low (solid line) and high (dashed line) inter-filament resistivity, respectively.

B. New Features of the Electromagnetic Input

The interpolative scaling from Durham University [24] was used for the Furukawa strand I_C , setting C_0 such as to recover the measured value of 154 A [10]. For the exponent n , the I_C -dependent scaling in [25] was used, with a cubic best fit of the normalized r factor as a function of the strain derived from the data presented there.

With reference to Table I, it should be noted that, above $\sim 0.7\%$, the Durham scaling predicts $I_C \sim 0$, i.e., all strand regions above this tensile value will not contribute to carry the current. Also, an irreversible strain level could be introduced ad hoc at even lower values and a crude approximation of the effects of fracture easily included in our model—resistive bridges automatically arising in this case—at least as far as no feed-back on the thermo-mechanics is foreseen. The treatment of these effects is however beyond the scope of the present work, also because no irreversibility data are available for the Furukawa strand at this time.

The transverse conductance between (adjacent) SEs was considered parametrically. Results below refer to the maximum (pure Cu) conductance. Lower conductance would lead to lower I_C (i.e., further away from measured values, see below).

Another parameter which can potentially affect the computed results is the conductance assumed between SEs and outer Cu annulus. However, the value in the following is fixed and was not, so far, considered in a sensitivity study.

IV. RESULTS AND DISCUSSION

A. Performance Degradation

A first, analytical estimate of the performance degradation due to bending can be obtained using the formulas of Ekin [26], in the low or high inter-filament resistivity limits, together with the computed strain maps of Section II (including the displacement of the neutral axis). It is shown in Fig. 5 that the measured

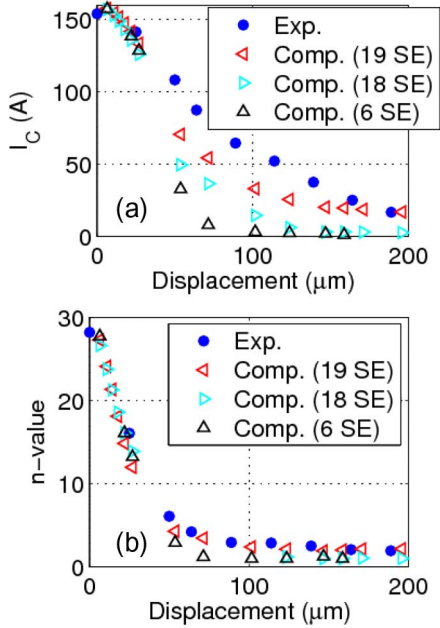


Fig. 6. Computed vs measured critical current I_C (a) and exponent n (b) as a function of displacement, for different discretizations of the filament region.

values fall between the two boundaries and closer to the low resistivity limit. This is similar to what was found in other strands [11] as well as in other recent analysis and tests of the same Furukawa strand [27].

The degradation of the performance of the strand computed together with the evolution of the current distribution among the SEs using the THELMA code is summarized in Fig. 6, in terms of both I_C and n . The agreement in I_C between simulation and experiment improves for increasingly refined discretizations, with an error of $\sim 30\%$ at intermediate displacements, while the agreement in n is good and much less sensitive to the discretization. These results constitute an improvement compared to the simulations presented in [19].

B. Current Non-Uniformity and Re-Distribution

As an example of what is inside the electro-magnetic part of the model, we report in Fig. 7 the computed evolution of the current in each SE, normalized to the respective (local) critical current, for $N_{SE} = 19$, in the case of zero and finite bending load, respectively. The initial phase of the transient is dominated by inductive effects. In the case without bending, the current starts flowing in the outermost layer of the filament region, then diffuses toward the center and the critical condition is reached uniformly over the strand cross section. In the case of a finite bending load, the current in the central SE initially flows opposite to the transport (total) current. As each SE approaches its critical current, redistribution occurs and progressively more SEs are involved as effective current carriers. Note however that the fraction of the outer SEs in the most severe strain conditions does not carry yet a significant current, even when critical conditions are reached in the wire (total transport current = I_C).

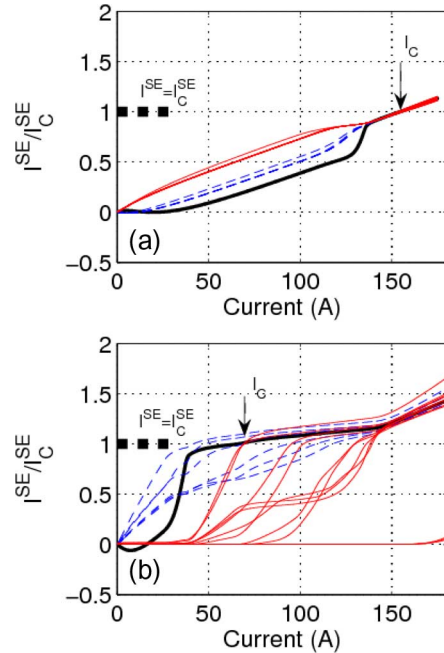


Fig. 7. Computed evolution of the current distribution (current I^{SE} normalized to the respective critical current) inside the strand. $N_{SE} = 19$, $z = 0.04$ m (mid-point) along the strand, section S0. a) $\delta = 0 \mu\text{m}$; b) $\delta = 53.7 \mu\text{m}$. Central SE (thick solid line), SEs in inner annulus (dashed lines), SEs in outer annulus (thin solid lines).

The non-uniform distribution will relax eventually to a uniform one, above I_C (not shown).

C. Effect of the Outer Cu Annulus

The calculations show that the outer Cu annulus plays an important role, at large values of the displacement. If the average voltage along the SEs was considered as in [19], instead than the average voltage along the strand surface as done here, then already at displacements $\geq 50 \mu\text{m}$ the corresponding I_C would drop to almost zero (not shown).

V. CONCLUSION

The hybrid thermo-mechanical-electromagnetic analysis of the performance of a single strand subject to bending [10], presented in [19], has been reconsidered here using improved model and input. The model has basically no ad hoc ingredients, such that it can be considered of predictive nature, for a well-characterized strand.

The agreement between simulated and measured degradation as a function of increasing bending load is reasonable both in terms of I_C and in terms of n .

Further improvement in the accuracy of the simulation could be expected by more realistic application of the bending load via a suitable contact algorithm, more flexible discretization of the strand cross section in the electromagnetic (THELMA) model, as well as from a parametric study of the effects of the conductivity between the filament region and the outer Cu annulus.

REFERENCES

- [1] H. Tsuji, K. Okuno, R. Thome, E. Salpietro, S. Egorov, N. Martovetsky, M. Ricci, R. Zanino, G. Zahn, A. Martinez, G. Vecsey, K. Arai, T. Ishigooka, T. Kato, T. Ando, Y. Takahashi, H. Nakajima, T. Hiyama, M. Sugimoto, N. Hosogane, M. Matsukawa, Y. Miura, T. Terakado, J. Okano, K. Shimada, M. Yamashita, T. Isono, N. Koizumi, K. Kawano, M. Oshikiri, Y. Nunoya, K. Matsui, Y. Tsuchiya, G. Nishijima, H. Kubo, T. Shimba, E. Hara, K. Imahashi, Y. Uno, T. Ohuchi, K. Ohtsu, J. Okayama, T. Kawasaki, M. Kawabe, S. Seki, K. Takano, Y. Takaya, F. Tajiri, F. Tsutsumi, T. Nakamura, H. Hanawa, H. Wakabayashi, T. Shimizu, K. Kuramochi, T. Omine, T. Tamiya, J. Harada, K. Nishii, M. Huguët, N. Mitchell, D. Bessette, J. Minervini, R. Vieira, P. Michael, M. Takayasu, G. Bevilacqua, R. K. Maix, R. Manahan, R. J. Jayakumar, L. Savoldi, W. Herz, and A. Ninomiya, "Progress of the ITER central solenoid model coil program," *Nucl. Fusion*, vol. 41, pp. 645–651, 2001.
- [2] A. Ulbricht, J. L. Duchateau, W. H. Fietz, D. Ciazynski, H. Fillunger, S. Fink, R. Heller, R. Maix, S. Nicolle, S. Raff, M. Ricci, E. Salpietro, G. Zahn, R. Zanino, M. Bagnasco, D. Bessette, E. Bobrov, T. Bonicelli, P. Bruzzone, M. S. Darweschad, P. Decool, N. Dolgetta, A. della Corte, A. Formisano, A. Gruenhagen, P. Hertout, W. Herz, M. Huguët, F. Hurd, Y. Ilyin, P. Komarek, P. Libeyre, V. Marchese, C. Marinucci, A. Martinez, R. Martone, N. Martovetsky, P. Michael, N. Mitchell, A. Nijhuis, G. Noether, Y. Nunoya, M. Polak, A. Portone, L. S. Richard, M. Spadoni, M. Suesser, S. Turtu', A. Vostner, Y. Takahashi, F. Wuechner, and L. Zani, "The ITER toroidal field model coil project," *Fus. Eng. Des.*, vol. 73, pp. 189–327, 2005.
- [3] R. Zanino, N. Mitchell, and L. S. Richard, "Analysis and interpretation of the full set (2000–2002) of Tes tests in conductor 1 A of the ITER central solenoid model coil," *Cryogenics*, vol. 43, pp. 179–197, 2003.
- [4] R. Zanino and L. S. Richard, TFMC Testing Group, "Performance evaluation of the ITER toroidal field model coil phase I. Part 1: current sharing temperature measurement," *Cryogenics*, vol. 43, pp. 79–90, 2003.
- [5] R. Zanino and L. S. Richard, "Performance evaluation of the ITER toroidal field model coil phase I. Part 2: M&M analysis and interpretation," *Cryogenics*, vol. 43, pp. 91–100, 2003.
- [6] N. Mitchell, "Analysis of the effect of Nb₃Sn strand bending on CICC superconductor performance," *Cryogenics*, vol. 42, pp. 311–325, 2002.
- [7] L. S. Richard, N. Mitchell, and R. Zanino, "From short sample to coil DC superconductor performance: ITER Central Solenoid Model Coil (CSMC) versus Good Joint (GJ) sample," *IEEE Trans. Appl. Supercond.*, vol. 16, pp. 799–802, 2006.
- [8] L. S. Richard, P. Bruzzone, N. Mitchell, P. L. Ribani, and R. Zanino, "Assessment of the effect of current non-uniformity on the ITER Nb₃Sn good joint short sample DC performance," *IEEE Trans. Appl. Supercond.*, vol. 17, pp. 1382–1385, 2007.
- [9] R. Zanino, D. Ciazynski, N. Mitchell, and L. S. Richard, "Coupled mechanical-electromagnetic-thermal-hydraulic effects in Nb₃Sn cable-in-conduit conductors for ITER," *Supercond. Sci. and Technol.*, vol. 18, pp. S376–S382, 2005.
- [10] Y. Nunoya, T. Isono, and K. Okuno, "Experimental investigation on the effect of transverse electromagnetic force on the V-T curve of the CIC conductor," *IEEE Trans. Appl. Supercond.*, vol. 14, pp. 1468–1472, 2004.
- [11] N. van den Eijnden, A. Nijhuis, Y. Ilyin, W. A. J. Wessel, and H. H. J. ten Kate, "Axial tensile stress strain characterisation of ITER model coil type Nb₃Sn strands in TARSIS," *Supercond. Sci. Technol.*, vol. 18, pp. 1523–1532, 2005.
- [12] K. P. Weiss, R. Heller, W. H. Fietz, J. L. Duchateau, N. Dolgetta, and A. Vostner, "Systematic approach to examine the strain effect on the critical current of Nb₃Sn cable-in-conduit-conductors," *IEEE Trans. Appl. Supercond.*, vol. 17, pp. 1469–1472, 2007.
- [13] P. Bruzzone, M. Bagnasco, M. Calvi, F. Cau, D. Ciazynski, A. della Corte, A. Di Zenobio, L. Muzzi, A. Nijhuis, E. Salpietro, L. S. Richard, S. Turtu', A. Vostner, R. Wesche, and R. Zanino, "Test results of two European ITER TF conductor samples in SULTAN," *IEEE Trans. Appl. Supercond.*, submitted for publication.
- [14] D. P. Boso, M. Lefik, and B. A. Schrefler, "Thermal and bending strain on Nb₃Sn strands," *IEEE Trans. Appl. Supercond.*, vol. 16, pp. 1823–1827, 2006.
- [15] D. P. Boso, M. Lefik, and B. A. Schrefler, "Homogenisation methods for the thermo-mechanical analysis of Nb₃Sn based strand," *Cryogenics*, vol. 46, pp. 569–580, 2006.
- [16] D. P. Boso, M. Lefik, and B. A. Schrefler, "Multiscale analysis of the influence of the triplet helicoidal geometry on the strain state of a Nb₃Sn based strand for ITER coils," *Cryogenics*, vol. 45, no. 9, pp. 589–605, 2005.
- [17] D. P. Boso, M. Lefik, and B. A. Schrefler, "A multilevel homogenised model for superconducting strands thermomechanics," *Cryogenics*, vol. 45, pp. 259–271, 2005.
- [18] M. Ciotti, A. Nijhuis, P. L. Ribani, L. S. Richard, and R. Zanino, "THELMA code electromagnetic model of ITER superconducting cables and application to the ENEA stability experiment," *Supercond. Sci. Technol.*, vol. 19, pp. 987–997, 2006.
- [19] P. L. Ribani, D. P. Boso, M. Lefik, Y. Nunoya, L. S. Richard, B. A. Schrefler, and R. Zanino, "THELMA code analysis of bronze route Nb₃Sn strand bending effect on I_c," *IEEE Trans. Appl. Supercond.*, vol. 16, pp. 860–863, 2006.
- [20] M. Hirohashi, H. Murakami, A. Ishiyama, H. Ueda, N. Koizumi, and K. Okuno, "Numerical simulation of the critical current and n-value in Nb₃Sn strand subjected to bending strain," *IEEE Trans. Appl. Supercond.*, vol. 16, pp. 1721–1724, 2006.
- [21] H. Murakami, A. Ishiyama, H. Ueda, N. Koizumi, and K. Okuno, "Numerical simulation of critical current and n-value in Nb₃Sn strand subjected to bending strain," *IEEE Trans. Appl. Supercond.*, vol. 17, pp. 1394–1397, 2007.
- [22] P. Bauer, H. Rajainmaki, and E. Salpietro, EFDA Material Data Compilation for Superconductor Simulation Apr. 2007, unpublished.
- [23] M. Breschi and P. L. Ribani, "Electromagnetic modeling of the jacket in cable in conduit conductors," *IEEE Trans. Appl. Supercond.*, submitted for publication.
- [24] D. M. J. Taylor and D. P. Hampshire, "The scaling law for the strain dependence of the critical current density in Nb₃Sn superconducting wires," *Supercond. Sci. Technol.*, vol. 18, pp. S241–S252, 2005.
- [25] D. M. J. Taylor and D. P. Hampshire, "Relationship between the n-value and critical current in Nb₃Sn superconducting wires exhibiting intrinsic and extrinsic behaviour," *Supercond. Sci. Technol.*, vol. 18, pp. S297–S302, 2005.
- [26] J. W. Ekin, "Mechanical properties and strain effects in superconductors," *Superconductor Material Sciences*, ch. 7, NATO ASI series, series B, Physics, 0068, pp. 455–510.
- [27] N. Koizumi, Y. Nabara, K. Matsui, and T. Hemme, "Strand bending tests at JAEA," in *ITER Conductor Meeting*, Villigen, Switzerland, Jul. 2007, unpublished.